Desalination and Water Treatment
www.deswater.com

doi: 10.1080/19443994.2016.1185746

57 (2016) 28378–28385
December

Taylor & Francis
Taylor & Francis Group

Enhancing sonocatalytic properties of TiO_2 nanocatalysts by controlling the surface conditions: effect of particle size and PVA modification

Foad Soleimani[a], Hamid Reza Madaah Hosseini[a,*], Farideh Ordikhani[a], Manijhe Mokhtari-Dizaji[b]

[a]*Department of Materials Science and Engineering, Sharif University of Technology, Azadi Ave., P.O. Box 11155-9466, Tehran, Iran, Tel. +98 912 7638727; Fax: +98 21 44659489; email: foadsoleimani@alum.sharif.edu (F. Soleimani), Tel. +98 21 66165258; Fax: +98 21 66005717; email: madaah@sharif.edu (H.R. Madaah Hosseini), Tel. +98 21 66165201; Fax: +98 21 66005717; email: faride.ordikhani@gmail.com (F. Ordikhani)*

[b]*Faculty of Medical Sciences, Department of Medical Physics, Tarbiat Modares University, Jalal Ale Ahmad Highway, P.O. Box 14115-111, Tehran, Iran, Tel. +98 21 82883893; Fax: +98 21 88006544; email: mokhtarm@modares.ac.ir*

Received 2 February 2016; Accepted 28 April 2016

ABSTRACT

The influence of particle size and surface modification on sonocatalytic activity of TiO_2 nanoparticles was investigated by measuring the degradation efficiency of methyl orange (MO) as a model pollutant. Crystalline TiO_2 nanoparticles with different particles and aggregate size were prepared through solution-phase method with varying synthesis temperatures. Coating with polyvinyl alcohol was performed to enhance colloidal stability of the particles over a wide range of pH values (1.5–7.5). Characterization was carried out using X-ray diffraction, high-resolution transmission electron microscopy, dynamic light scattering, and Fourier-transformed infrared techniques. It was found that sonodegradation of MO decreased as the synthesis temperature increased. Moreover, sonoactivity of the modified nanoparticles improved because polymeric coating inhibited particles collision and also their growth due to sonication-induced Ostwald ripening mechanism.

Keywords: TiO_2 nanoparticles; Aggregate size; Sonocatalytic properties; Colloidal stability; Polyvinyl alcohol; Wastewater treatment

1. Introduction

TiO_2 particles have been extensively explored for their catalytic applications especially in environmental treatment, self-cleaning surfaces, bactericidal activity, and cancer therapy [1–6]. Photocatalytic properties of TiO_2 originate from generation of reactive oxygen species (ROS) such as hydroxyl radical (·OH) under illumination of ultraviolet (UV) light [3,4,7]. Two well-known ways to enhance the photocatalytic properties are to prepare ultrafine particles with large surface areas and to improve their colloidal stability [1,5–12]. Studies on the effect of TiO_2 particle size on its photocatalytic activity show that the best catalytic properties are mainly obtained at an optimal size [7–9,13]. However, there are significant disagreements in the reported results, more likely due to the different preparation techniques and the less-considered effect of aggregate size on photoactivity [1,8,9].

*Corresponding author.

Recent studies have shown that irradiation with ultrasound (US) waves rather than UV light can result in much better catalytic properties [6,14–16]. Local sonoluminescence and hot spots caused by acoustic cavitation provide high energies sufficient to activate the semiconductors [3,14]. As US waves can penetrate in water medium easily, applying these waves offers more benefits in wastewater treatment [15]. To the best of the authors' knowledge, the effect of particle size on sonocatalytic properties of TiO_2 nanoparticles has not been considered yet.

In this work, TiO_2 nanoparticles were prepared via the root of solution-phase synthesis. Nanocolloidal particles were formed through the hydrolysis and condensation of titanium alkoxide in aqueous medium [11,17–19]. Polyvinyl alcohol (PVA) as a hydrophilic polymer was used to modify the surface of nanoparticles. Polymer chains can keep nanoparticles away from agglomeration and colloidal instability, particularly at near neutral pH values [6,20–25]. Sonocatalytic properties of TiO_2 nanoparticles were studied as a function of particle size and compared with the properties of PVA-coated nanoparticles.

2. Experimental

2.1. Chemicals, sol preparation, and surface modification

Titanium tetraisopropoxide (TTIP) (≥98%, Merck) as precursor, analytical grade of hydrochloric acid (HCl) 37% (density of 1.19 g/cm^3, Merck) as both catalyst and peptizing agent, and deionised (DI) water as dispersing media were used to synthesize TiO_2 nanoparticles in the following procedure.

A proper amount of acidified water was magnetically stirred in a sealed multineck flask placed in a temperature-controlled bath. The mixture was stabilized at desired temperature and then TTIP was added under constant magnetic stirring at 140 rpm. White flocs immediately formed all over the media as a result of hydrolysis and condensation reactions. The mixture was refluxed for 12 h to ensure that equilibrium between peptization and reaggregation stages was reached. The resulted colloid was translucent, with a characteristic bluish color. Then, the mixture was slowly cooled down to room temperature under continuous stirring.

For surface modification, dry PVA (Mw = 72,000, degree of hydrolysis ≥97%, Merck) was dissolved in DI-water. The colloid of nanoparticles was slowly added and mixed with the PVA solution using a magnetic stirrer. PVA concentration and mixing duration were kept to optimum values in order to obtain the most stable sols in pH range of 1.5–7.5. Reagent grade NaOH (1 M) and HCl (0.2 M) were used to adjust the pH value of the sols to near neutral pH. The stability of sols was qualitatively checked over one month using a Mi-415 turbidimeter (Martini Instruments, USA) based on light absorbance of modified nanoparticles. Synthesis parameters and modification processing details are presented in Table 1.

2.2. Characterization methodology

X-ray diffraction (XRD) data of the dried bare nanoparticles were recorded on a STOE Stadi-P diffractometer (Cu-K_α radiation, 40 kV, 30 mA). Crystalline silicon powder (325 mesh, Aldrich) was used to determine the instrument broadening (β) of peaks, which was about 0.18° (2θ). High-resolution transmission electron microscopy (HRTEM) analyses were carried out on a JEM-2100 HRTEM (JEOL, USA) with an accelerating voltage of 200 kV. In sample preparation procedure, a proper amount of diluted sol (~1 ppm) was mixed with high purity ethanol in 1:1 volume ratio. Then, one drop was placed onto a copper grid coated with amorphous carbon film and let to dry under ambient conditions. In the case of PVA-coated nanoparticles, the sample was stained by phosphotungstic acid. Aggregate size measurements were conducted via dynamic light scattering (DLS) analysis with a Zetasizer Nano-S (Malvern Instruments Ltd, UK). Fourier-transformed infrared (FT-IR) spectra of the samples were recorded using a Shimadzu-8400S FT-IR spectrometer. FT-IR samples were prepared through mixing and grounding with potassium bromide (KBr) and then pressed into a pellet.

2.3. Sonocatalytic reactivity experiments

An appropriate amount of high concentration methyl orange (MO) aqueous solution (dye-to-particle mass ratio = 1/100) was added to each sol ([TiO_2] = 2 g/L). The resulting suspension was magnetically stirred for 30 min to reach the equilibrium state of dye adsorption/desorption. Five milliliters of the colloid was withdrawn for UV–vis spectroscopy and 30 ml poured into a closed container with a perforated lid. A flat tip TT13 sonifier probe was introduced into the center of the sol. The reaction vessel was then placed inside a water bath to keep the temperature at around 25°C, and the sample was exposed to US waves provided by an ultrasonic processor (Bandelin SONOPULS HD-3200, frequency = 20 kHz, output power = 50 W) for 30 min with 5 s on and 5 s off pulsation. The dye concentrations were determined from the visible spectra recorded in the range of 400–700 nm using a PerkinElmer Lambda-25 UV–visible spectrometer.

Table 1
Processing parameters used in the synthesis and modification steps

	As-synthesized nanoparticles			PVA-modified nanoparticles		
Synthesis temperature (°C)	Sol name	$[H_2O]:[Ti]:[H^+]$	Duration (h)	Sol name	TiO_2/PVA (g/g)	Duration (h)
50 ± 2	G50	116:1:0.5	12	G50P	2.7	4
70 ± 2	G70	116:1:0.5	12	G70P	2.7	4
90 ± 2	G90	116:1:0.5	12	G90P	2.7	4

3. Results and discussion

3.1. Nanoparticles characterization

Fig. 1 shows XRD patterns of TiO_2 nanoparticles synthesized at 50, 70, and 90°C. The major phase in the synthesized particles is anatase, and brookite is the minor phase [11,17–19]. Relative amounts of the present phases were estimated by dividing the integrated area under anatase (0 0 4) reflection at $2\theta = 37.8^\circ$ to that of brookite (1 2 1) at $2\theta = 30.8^\circ$. The results were 1.3, 1.2, and 1.2 for the samples G50, G70, and G90, respectively. So, the synthesis temperature had a slight effect on the quality of the phases. Since both anatase and brookite phases could contribute in photoactivity [26], all of the diffracted peaks were considered in crystallite size calculations. The average crystallite size was calculated using the Scherrer formula, $D = k\lambda/(B\cos\theta)$, where D is the particle diameter, k is a constant (0.90), λ is the X-ray wavelength (1.54 Å for Cu-K_α), B (in radians) is the full-width at half maximum (FWHM), and θ (in degrees) is the angle of the diffracted peak [7,11]. The parameter B is calculated as $B = b - \beta$, where b is the experimental FWHM and β is the instrumental broadening.

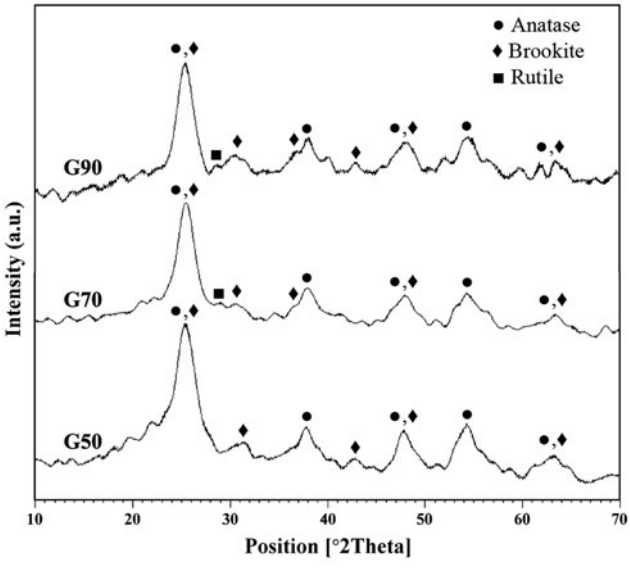

Fig. 1. XRD patterns of titania nanoparticles synthesized via solution-phase method at 50 (G50), 70 (G70), and 90°C (G90).

Fig. 2 shows HRTEM images for the samples G50P, G70, and G90. Both the primary particle and aggregate size increased by increasing the synthesis temperature, which the latter occurred more intensely [18]. The growth of the primary particles is dominated by diffusion-limited coarsening, known as Ostwald ripening (OR) which occurs easier at elevated temperatures. A second coarsening mechanism is oriented attachment of primary particles, which may happen under wide range of processing conditions [11,12]. So, the resulting secondary particles had irregular shapes and were bimodal-sized (Fig. 2(b) and (c)). The average primary particle size calculated from HRTEM images and XRD data are listed in Table 2. The particle size calculated from XRD patterns is a factor of 1.5–2 larger than that obtained from HRTEM images [11].

By staining, the organic coating of modified nanoparticles became visible on TEM images (Fig. 2(a) and (d)). PVA is responsible for image blurring due to film formation [20,21]. There are areas darker than background and brighter than particles around and between the aggregates, pertaining to stained polymer chains. The insets in Fig. 2(d), (e), and (f) show SAED patterns for each sample in which the main rings from the beginning are consistent with anatase (1 0 1), brookite (1 2 1), anatase (0 0 4), anatase (2 0 0), anatase (2 1 1), and anatase (2 0 4) planes, respectively. It is concluded that fully crystalline nanopowders were synthesized. The shift of the crystalline diffraction pattern toward amorphous pattern in sample G50P could be attributed to the polymer surrounding the particles.

Although higher temperature causes the peptizing agent to fragment the agglomerates, it may result in higher mobility, enhancing the probability of particles collision and thus gives rise to aggregation of the particles [18,19]. Therefore, it is most likely to obtain bimodal aggregates at higher temperatures, as seen in Fig. 3. The Z-average size obtained from

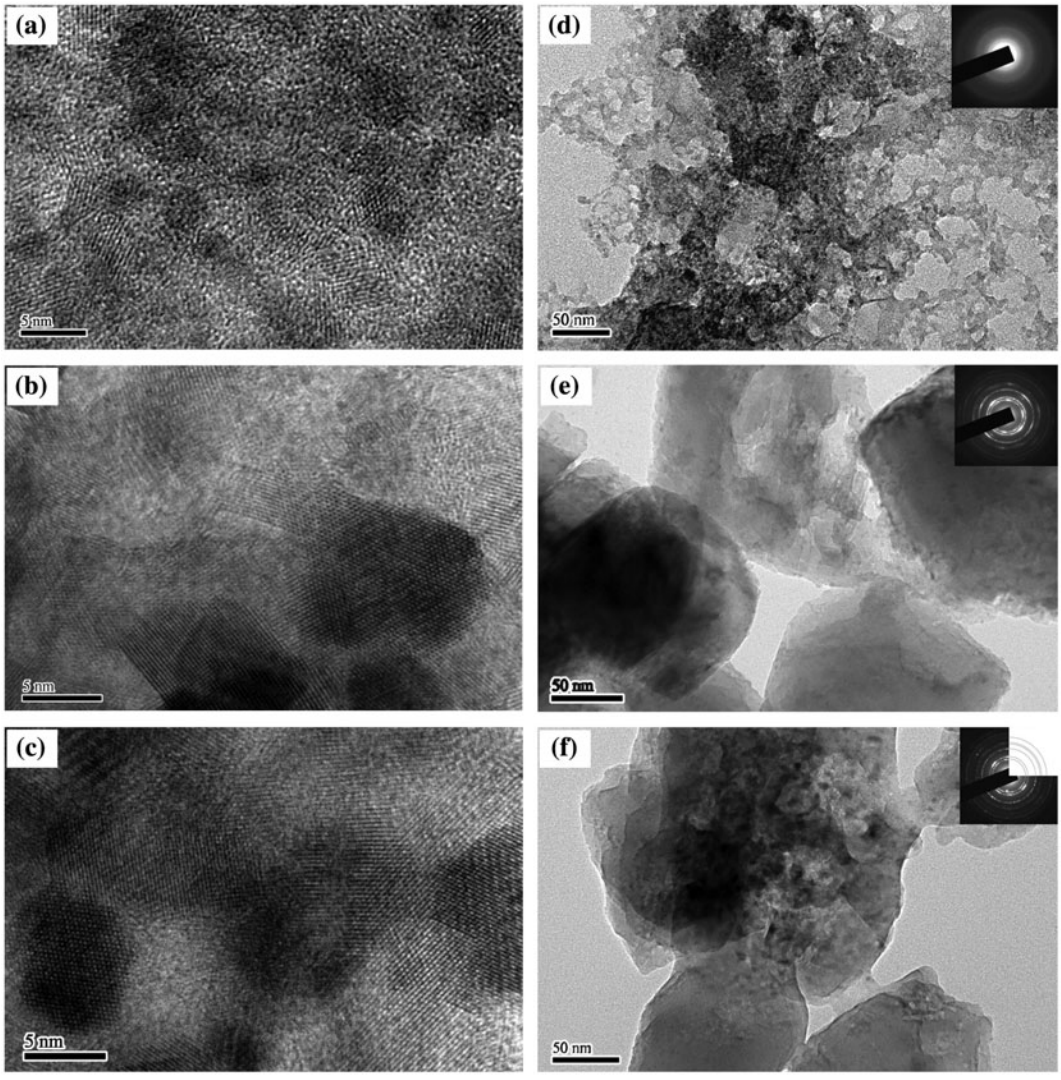

Fig. 2. HRTEM images of (a, d) TiO_2 nanoparticles synthesized at 50˚C and modified with PVA, (b, e) nanoparticles synthesized at 70˚C, and (c, f) nanoparticles synthesized at 90˚C: (a, b, c) represents primary particles; (d, e, f) represents aggregates formed by nanoparticles.

Table 2
Particle size analyses by various techniques

Sample name	Crystallite size[a]	Particle size[b]	Aggregate size[c]
G50	10.8	6.8 ± 0.5	20.1
G70	12.4	8.1 ± 0.5	31.0
G90	14.0	8.7 ± 0.5	39.3

[a]Calculated average particle size (nm) by applying Scherrer formula on all diffracted peaks of XRD patterns.
[b]Average primary particle diameter (nm) based on HRTEM observations.
[c]Average hydrodynamic size of aggregate (Z-average size) based on DLS measurements (nm).

DLS data (Table 2) reveals that the average hydrodynamic diameter increased at higher temperatures even though smaller monomodal aggregates were synthesized.

3.2. Surface modification

FT-IR spectra of pristine nanoparticles, pure PVA, and PVA-modified nanoparticles are shown in Fig. 4.

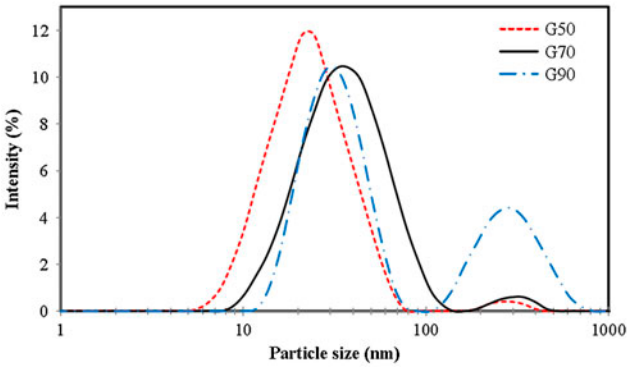

Fig. 3. Aggregates hydrodynamic diameter measurements using DLS method for the bare nanoparticles synthesized at 50 (G50), 70 (G70), and 90°C (G90).

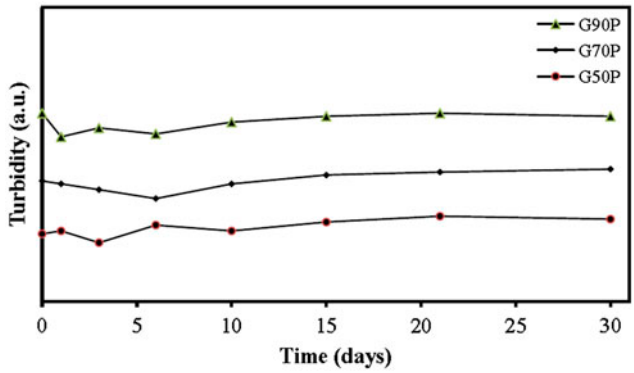

Fig. 5. Turbidity of PVA-coated TiO_2 nanoparticles sols at near neutral pH.

For comparison, the spectrum of pure water is provided in Fig. 4(a). The broad peaks around 3,170 and 1,616 cm^{-1} in Fig. 4(b) correspond to the vibrations of hydroxyl groups and water molecules adsorbed on the surface of titania nanoparticles [25,27,28]. However, the observed bands are quite different from those in Fig. 4(c), which are attributed to intermolecular and intramolecular hydrogen bonds [29]. PVA could also absorb water molecules to some extents [30]. In the spectrum of PVA-coated nanoparticles, the characteristic bands of hydroxyl groups shifted to larger wavenumbers. Furthermore, the peaks assigned to $–CH_2$ and –CH groups shifted comparing with the pure polymer spectrum, which verified that PVA was attached to titania via hydrogen bonding between its polar functional groups and the hydroxylated and protonated surface of the oxide [21].

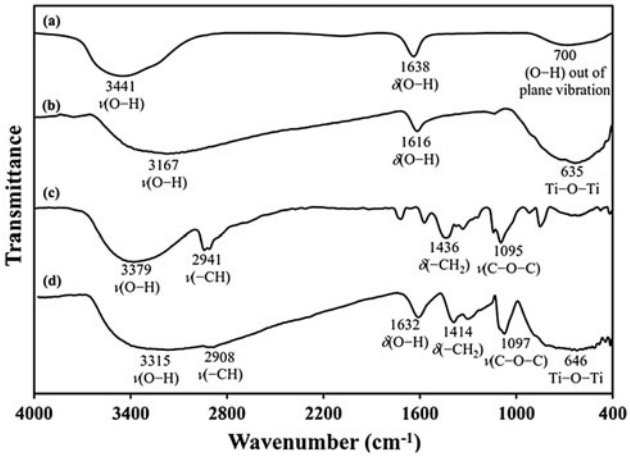

Fig. 4. FT-IR spectra of (a) pure water, (b) TiO_2 nanoparticles, (c) neat PVA, and (d) PVA-coated TiO_2 nanoparticles.

The room temperature isoelectric point of nanocrystalline anatase is in pH range of 5–7 [12]. Since the pH of titania sols was around 1.5, stability of the sols was achieved by electrostatic repulsion due to surface charges [18]. By increasing the pH toward isoelectric point, uncharged nanoparticles tend to coagulate and coalesce due to van der Waals attractions [1,19,31]. The results of turbidimetry (Fig. 5) show that PVA coating could provide a well-defined barrier between the particles by steric stabilization mechanism. A good stability was achieved for the sols containing PVA-coated nanoparticles over a month after adjusting their pH at around neutral value.

3.3. Sonocatalytic activity

Study on degradation of organic dyes in an aqueous solution is a facile method to evaluate the sonocatalytic properties of catalysts [2,3,15]. The MO concentrations before and after US irradiation were measured from the characteristic absorption peak at 495 nm in the relevant spectra. By comparing these intensities, the degradation efficiency would be determined. Most of the MO molecules initially adsorbed to the TiO_2 surface desorb immediately under ultrasonication and, hence, the initial adsorption amount can be omitted [15].

Fig. 6 depicts sonocatalytic degradation of MO as functions of primary particle and aggregate size. Effect of US on dye degradation was also examined for a solution without nanoparticles. In the presence of TiO_2 as a sonosensitizer, degradation efficiency of the dye gradually decreased as particle size increased. Previous studies indicated that photodegradation rate roughly decreased by a factor of 1.2 when primary particle size increased from 3.8 to 5.7 nm [7] and by a factor of 1.3 when primary particle size increased from 7

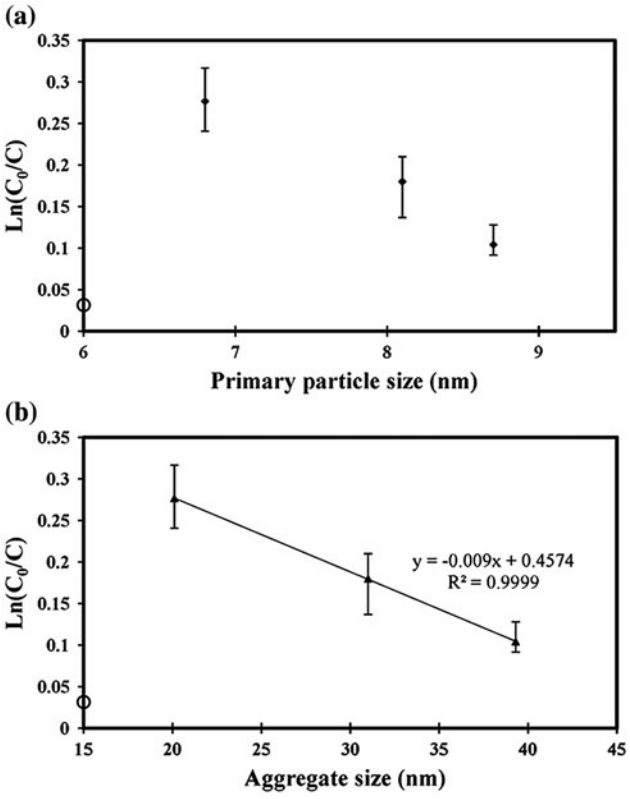

Fig. 6. Sonocatalytic degradation of MO in the presence of bare TiO_2 nanoparticles: (a) as a function of their primary particles size and (b) as a function of their aggregates size. The mark ○ pertains to the sample of dye solution without nanoparticles. C_0 is the initial concentration and C is the concentration of the MO after 30-min irradiation (mg/L).

to 11 nm [8]. Fig. 6(a) demonstrates that by slight increase of the primary particle size from 6.8 to 8.7 nm, the degradation rate diminished by a significant factor of 2.7. Moreover, Fig. 6(b) suggests that size variation of the aggregates impressed the sonocatalytic properties of TiO_2 significantly. The observed linear correlation between degradation rate and the aggregates size is in accord with previous findings on the effects of aggregate size on photocatalytic degradation of trichloroethylene [8]. Therefore, sonoactivity decreased markedly due to the particles aggregation, while part of the observed variations in the properties arose from different primary particle sizes.

The very proximity of particles' surfaces as the essential places for generation of ROS affects the local concentration of them. Electrons and holes on adjacent primary particles within an aggregate may quench each other, and free ·OH radicals recombine with either electrons or holes on the surfaces, increasing quenching. Additionally, the quantity of exciting photons reaching the particles within aggregates is in an inverse relationship with the aggregate size due to particle shadowing. This could intensify scattering of the incident light which largely depends on the size of the constitutive primary particles [1,7,8].

Fig. 7 schematically shows MO degradation ratio for modified and bare nanoparticles synthesized at 50, 70, and 90˚C. Diffusion of the species dissolved at the surface of some particles and rapid recrystallization of them on the others befall more easily in a colloid irradiated by US. Subsequently, larger particles grow at the expense of smaller particles (OR) [32]. Moreover, despite the dispersing effect of US waves on nanoparticles in a suspension, shock waves generated by cavitation may cause the particles to collide at relatively high velocities. The small particles are more involved in this type of collision [33]. The temperature produced in the localized hot spots is high enough to spot-weld the particles at the point of impact upon collision [34]. Therefore, the bare particles could reagglomerate and form an aggregate even larger than the initial one under the US irradiation. Reagglomeration and particle growth due to OR phenomenon are expected to be effectively hindered in the coated nanoparticles, and distribution of the particles was improved [35], resulting in enhancement of sonocatalytic properties.

This positive effect of the coating was preserved as long as it was not a deterrent for dye adsorption on the particles surfaces [36]. For larger particles, more polymeric chains were in contact with the surface of them since the polymer-to-nanoparticle mass ratio was invariant in all three samples. So, reduction of sonocatalytic degradation efficiency was faster in the modified nanoparticles in comparison with the bare ones, as evidenced in Fig. 7.

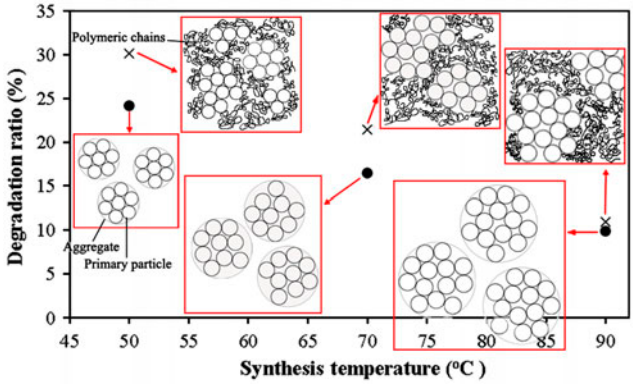

Fig. 7. Schematic representation for influence of synthesis temperature on the sonocatalytic degradation efficiency of MO for unmodified (●) and modified (×) nanoparticles.

4. Conclusions

Electrostatically stable TiO_2 nanoparticles in an aqueous media were obtained through the facile method of solution-phase synthesis. Keeping other parameters constant, synthesis temperature varied from 50 to 90˚C. Results revealed that increasing the synthesis temperature increased aggregate size more intensely than average primary particle size. Sonocatalytic efficacy of the prepared nanoparticles decreased as the synthesis temperature increased predominantly due to pronounced effect of aggregates enlargement on charge carriers quenching and particle shadowing. Furthermore, sonoactivity was enhanced in PVA-modified nanoparticles. PVA could inhibit the reaggregation/agglomeration of the particles in the sonicated media and the subsequent reduction in effective surface area. Surface modification led to more stability of the nanoparticles over a wide range of pH values as a consequence of establishment of hydrogen bonds between polymeric coating and hydroxylated surface of the particles. Polymer coating retarded the particle growth due to sonication-induced OR mechanism.

Acknowledgments

The authors would like to acknowledge the financial support from Iran Nanotechnology Initiative Council (INIC).

References

[1] D. Jassby, J.F. Budarz, M. Wiesner, Impact of aggregate size and structure on the photocatalytic properties of TiO_2 and ZnO nanoparticles, Environ. Sci. Technol. 46 (2012) 6934–6941.
[2] A.Z. Abdullah, P.Y. Ling, Heat treatment effects on the characteristics and sonocatalytic performance of TiO_2 in the degradation of organic dyes in aqueous solution, J. Hazard. Mater. 173 (2010) 159–167.
[3] J. Wang, Y. Guo, B. Liu, X. Jin, L. Liu, R. Xu, Y. Kong, B. Wang, Detection and analysis of reactive oxygen species (ROS) generated by nano-sized TiO_2 powder under ultrasonic irradiation and application in sonocatalytic degradation of organic dyes, Ultrason. Sonochem. 18 (2011) 177–183.
[4] N. Ertugay, F.N. Acar, Decolorization of direct blue 71 using UV irradiation and ultrasound in the presence of TiO_2 catalysts, Desalin. Water Treat. 57 (2016) 9318–9324.
[5] T. Sugimoto, X. Zhou, A. Muramatsu, Synthesis of uniform anatase TiO_2 nanoparticles by gel–sol method: 3. Formation process and size control, J. Colloid Interface Sci. 259 (2003) 43–52.
[6] S. Yamaguchi, H. Kobayashi, T. Narita, K. Kanehira, S. Sonezaki, N. Kudo, Y. Kubota, S. Terasaka, K. Houkin, Sonodynamic therapy using water-dispersed TiO_2-polyethylene glycol compound on glioma cells: Comparison of cytotoxic mechanism with photodynamic therapy, Ultrason. Sonochem. 18 (2011) 1197–1204.
[7] H. Lin, C.P. Huang, W. Li, C. Ni, S.I. Shah, Y.H. Tseng, Size dependency of nanocrystalline TiO_2 on its optical property and photocatalytic reactivity exemplified by 2-chlorophenol, Appl. Catal. B: Environ. 68 (2006) 1–11.
[8] A.J. Maira, K.L. Yeung, C.Y. Lee, P.L. Yue, C.K. Chan, Size effects in gas-phase photo-oxidation of trichloroethylene using nanometer-sized TiO_2 catalysts, J. Catal. 192 (2000) 185–196.
[9] K. Kočí, L. Obalová, L. Matějová, D. Plachá, Z. Lacný, J. Jirkovský, O. Šolcová, Effect of TiO_2 particle size on the photocatalytic reduction of CO_2, Appl. Catal. B: Environ. 89 (2009) 494–502.
[10] D.L. Liao, G.S. Wu, B.Q. Liao, Zeta potential of shape-controlled TiO_2 nanoparticles with surfactants, Colloids Surf. A: Physicochem. Eng. Aspects 348 (2009) 270–275.
[11] G. Oskam, A. Nellore, R.L. Penn, P.C. Searson, The growth kinetics of TiO_2 nanoparticles from titanium (IV) alkoxide at high water/titanium ratio, J. Phys. Chem. B 107 (2003) 1734–1738.
[12] R.L. Penn, J.F. Banfield, Morphology development and crystal growth in nanocrystalline aggregates under hydrothermal conditions: Insights from titania, Geochim. Cosmochim. Acta 63 (1999) 1549–1557.
[13] C.B. Almquist, P. Biswas, Role of synthesis method and particle size of nanostructured TiO_2 on its photoactivity, J. Catal. 212 (2002) 145–156.
[14] N. Shimizu, C. Ogino, M.F. Dadjour, K. Ninomiya, A. Fujihira, K. Sakiyama, Sonocatalytic facilitation of hydroxyl radical generation in the presence of TiO_2, Ultrason. Sonochem. 15 (2008) 988–994.
[15] J. Wang, B. Guo, X. Zhang, Z. Zhang, J. Han, J. Wu, Sonocatalytic degradation of methyl orange in the presence of TiO_2 catalysts and catalytic activity comparison of rutile and anatase, Ultrason. Sonochem. 12 (2005) 331–337.
[16] P. Singh, M.C. Vishnu, K.K. Sharma, R. Singh, S. Madhav, D. Tiwary, P.K. Mishra, Comparative study of dye degradation using TiO_2-activated carbon nanocomposites as catalysts in photocatalytic, sonocatalytic, and photosonocatalytic reactor, Desalin. Water Treat. (2015) 1–13, doi: 10.1080/19443994.2015.1108871.
[17] D. Vorkapic, T. Matsoukas, Reversible agglomeration: A kinetic model for the peptization of titania nanocolloids, J. Colloid Interface Sci. 214 (1999) 283–291.
[18] D. Vorkapic, T. Matsoukas, Effect of temperature and alcohols in the preparation of titania nanoparticles from alkoxides, J. Am. Ceram. Soc. 81 (1998) 2815–2820.
[19] M.C. Cordero-Cabrera, G.S. Walker, D.M. Grant, Effect of processing parameters on the particle size and stabilisation of titania sols, J. Mater. Sci. 40 (2005) 3709–3714.
[20] M. Chastellain, A. Petri, H. Hofmann, Particle size investigations of a multistep synthesis of PVA coated superparamagnetic nanoparticles, J. Colloid Interface Sci. 278 (2004) 353–360.
[21] S. Kayal, R.V. Ramanujan, Doxorubicin loaded PVA coated iron oxide nanoparticles for targeted drug delivery, Mater. Sci. Eng. C 30 (2010) 484–490.

[22] J. Lee, J. Hong, D.W. Park, S.E. Shim, Microencapsulation and characterization of poly (vinyl alcohol)-coated titanium dioxide particles for electrophoretic display, Opt. Mater. 32 (2010) 530–534.
[23] L. Körösi, S. Papp, I. Bertóti, I. Dékány, Surface and bulk composition, structure, and photocatalytic activity of phosphate-modified TiO_2, Chem. Mater. 19 (2007) 4811–4819.
[24] J. Zhao, M. Milanova, M.M.C.G. Warmoeskerken, V. Dutschk, Surface modification of TiO_2 nanoparticles with silane coupling agents, Colloids Surf. A: Physicochem. Eng. Aspects 413 (2012) 273–279.
[25] Y. Qu, W. Wang, L. Jing, S. Song, X. Shi, L. Xue, H. Fu, Surface modification of nanocrystalline anatase with CTAB in the acidic condition and its effects on photocatalytic activity and preferential growth of TiO_2, Appl. Surf. Sci. 257 (2010) 151–156.
[26] M. Addamo, M. Bellardita, A.D. Paola, L. Palmisano, Preparation and photoactivity of nanostructured anatase, rutile and brookite TiO_2 thin films, Chem. Commun. 47 (2006) 4943–4945.
[27] D. Zhao, C. Chen, Y. Wang, H. Ji, W. Ma, L. Zang, J. Zhao, Surface modification of TiO_2 by phosphate: Effect on photocatalytic activity and mechanism implication, J. Phys. Chem. C 112 (2008) 5993–6001.
[28] H. Li, C.P. Tripp, Interaction of sodium polyacrylate adsorbed on TiO_2 with cationic and anionic surfactants, Langmuir 20 (2004) 10526–10533.
[29] H.S. Mansur, C.M. Sadahira, A.N. Souza, A.A.P. Mansur, FTIR spectroscopy characterization of poly (vinyl alcohol) hydrogel with different hydrolysis degree and chemically crosslinked with glutaraldehyde, Mater. Sci. Eng. C 28 (2008) 539–548.
[30] Z.H. Ping, Q.T. Nguyen, S.M. Chen, J.Q. Zhou, Y.D. Ding, States of water in different hydrophilic polymers—DSC and FTIR studies, Polymer 42 (2001) 8461–8467.
[31] C.H. Yu, K. Tam, E.S.C. Tsang, Chemical methods for preparation of nanoparticles in solution, Handb. Met. Phys. 5 (2008) 113–141.
[32] J.A. Thompson, K.W. Chapman, W.J. Koros, C.W. Jones, S. Nair, Sonication-induced Ostwald ripening of ZIF-8 nanoparticles and formation of ZIF-8/polymer composite membranes, Microporous Mesoporous Mater. 158 (2012) 292–299.
[33] S.J. Doktycz, K.S. Suslick, Interparticle collisions driven by ultrasound, Science 247 (1990) 1067–1069.
[34] T. Fujimoto, S. Terauchi, H. Umehara, I. Kojima, W. Henderson, Sonochemical preparation of single-dispersion metal nanoparticles from metal salts, Chem. Mater. 13 (2001) 1057–1060.
[35] Z. Guo, D. Zhang, S. Wei, Z. Wang, A.B. Karki, Y. Li, P. Bernazzani, D.P. Young, J.A. Gomes, D.L. Cocke, T.C. Ho, Effects of iron oxide nanoparticles on polyvinyl alcohol: Interfacial layer and bulk nanocomposites thin film, J. Nanopart. Res. 12 (2010) 2415–2426.
[36] E. Ukaji, T. Furusawa, M. Sato, N. Suzuki, The effect of surface modification with silane coupling agent on suppressing the photo-catalytic activity of fine TiO_2 particles as inorganic UV filter, Appl. Surf. Sci. 254 (2007) 563–569.